JOURNAL OF SOLID STATE CHEMISTRY **129,** 37–44 (1997)
ARTICLE NO. SC967211

Nonaqueous Synthesis and Characterization of a New 2-Dimensional Layered Aluminophosphate $[Al_3P_4O_{16}]^{3-} \cdot 3[CH_3CH_2NH_3]^+$

Qiuming Gao, Baozong Li, Jiesheng Chen, Shougui Li, and Ruren Xu

Key Laboratory of Inorganic Hydrothermal Synthesis, Department of Chemistry, Jilin University, Changchun 130023, People's Republic of China

and

Ian Williams, Jiaqi Zheng, and David Barber

Department of Chemistry and Materials Characterization and Preparation Center, Hong Kong University of Science and Technology, Hong Kong

Received July 5, 1996; in revised form October 25, 1996; accepted October 30, 1996

The compound $[Al_3P_4O_{16}]^{3-} \cdot 3[CH_3CH_2NH_3]^+$ has been synthesized from the nonaqueous system H_3PO_4–$(i\,PrO)_3Al$–$CH_3CH_2NH_2$–$CH_3(CH_2)_3OH$. It has been definitively characterized by single-crystal X-ray diffraction, with space group $P2_1/m$ and unit cell $a = 8.920(2)$, $b = 14.896(2)$, $c = 9.363(2)$ Å, $\beta = 106.07(2)°$, and $V = 1191.6(4)$ Å^3. The structure consists of $[Al_3P_4O_{16}]^{3-}$ sheets with a $4 \times 6 \times 8$ network. This contains individual AlO_4 and PO_4 centered tetrahedral in the ratio of 3/4, in which all AlO_4 vertices are shared but each PO_4 has one terminal P=O. These are projected alternatively above and below the 2-D sheet and are hydrogen bonded to the ethylammonium ions which serve to template the structure. They give rise to elliptical eight-membered rings, which have a cavity size of 3.8×6.0 Å and an *AAAA* stacking sequence. This compound thus strengthens the family of $4 \times 6 \times 8$ and $4 \times 6 \times 12$ nets with *AAAA* or *ABAB* stackings for $[Al_3P_4O_{16}]^{3-}$, allowing rationalization based on the amine template length and functional multiplicity. Additional characterizations of the compound by XRD, SEM, IR spectroscopy, inductive coupled plasma analysis, TGA, and DTA are also described. © 1997 Academic Press

INTRODUCTION

Since Bibby and Dale (1) prepared silica-sodalite in ethylene glycol or propanol solvent, several zeolites or aluminophosphate molecular sieves with known or novel structures (2–5) have been synthesized in organic media, such as $AlPO_4$-5, $AlPO_4$-11 (2), and $AlPO_4$-17 (3), which have known structures, whereas JDF-2 (4) and JWD-12 (5) adopt novel structures. Structurally, most $AlPO_4$-*n* phases are exclusively composed of PO_4 and AlO_4 primary building units although a few contain AlO_5 and AlO_6 units. Recently, scientists have synthesized layered aluminophosphates with different P/Al ratios, e.g., P/Al ratios of 3/2 (6) and 4/3 (7–11) with a variety of ring sizes within the layer. The size of the rings and their stacking sequences can result in microporosity in some of these materials. Nonaqueous techniques have also been successfully used for the synthesis of ultralarge pore molecular sieves JDF-20 (12) and cloverite (13), giant crystals of zeolites and molecular sieves (14), and other known or novel 1-D, 2-D, and 3-D structural materials (15, 16), opening up vast vistas for nonaqueous synthesis. Here, we report the preparation of a new 2-D layered aluminophosphate $[Al_3P_4O_{16}]^{3-} \cdot 3[CH_3CH_2NH_3]^+$ (APO-TE) using the mixture of $CH_3(CH_2)_3OH$ and $HOCH_2CH_2OH$ as the medium and the characterization and structural elucidation of this compound.

EXPERIMENTAL

Synthesis and Characterization

Aluminum triisopropoxide and phosphoric acid (85% (weight)) were exclusively used as the aluminum and phosphorus sources. Thus aluminum triisoproposide (2.0 g) was added to the mixture of ethylene glycol (EG) (15.0 ml) and *n*-butanol (*n*-BuOH) (25.0 ml), then ethylamine (10 ml 75% (weight)) was added, and then phosphoric acid (2.0 ml) was added dropwise. The whole mixture was stirred until homogenous, sealed in a Teflon-lined autoclave (10 ml) with the filling rate about 70% (volume), and heated to 180°C for 13 days under autogenous conditions. Upon recovery from the mother liquor by vacuum filtration and after being washed with distilled water and dried at ambient temperature, the solid material (2.2 g) was recovered.

Elemental analysis was performed on a Perkin–Elmer 240C element analyzer. Scanning electron micrographs were taken on a Hitachi X-650B electron microscope. Inductive coupled plasma analysis (ICP) was conducted on a Jarrzall-ash 800 Mark-II ICP instrument. The IR

0022-4596/97 $25.00

measurements were carried out on a Nicolet 5DX FTIR spectrometer using KBr pellets. A Perkin–Elmer DTA 1700 differential thermal analyzer was used to conduct the differential thermal analysis (DTA) and a Perkin–Elmer TGA 7 thermogravimetric analyzer was used to obtain the thermogravimetric analysis (TGA) curve in air with the temperature increasing rate of 20°C min^{-1}.

Determination of Crystal Structure

Details of the crystal structure analysis are given in Table 1. A colorless crystal of APO-TE with approximate dimensions $100 \times 50 \times 50$ μm was selected. Data were collected using Mo$K\alpha$ radiation ($\lambda = 0.71073$ Å), on a Siemens P4-RA diffractometer at 295 K. A total of 3293 reflection intensities were measured to 2θ max 47.0° of which 1784 were symmetry independent and 1348 considered observed ($F > 4\ \sigma(F)$). Systematic absences of $0k0$, $k = 2n + 1$, were considered with either space group $P2_1$ or $P2_1/m$. The structure was solved in the centrosymmetric choice of $P2_1/m$ by direct methods and refined successfully by full-matrix least-squares to give final discrepancy indices of $R = 0.036$, $R_w = 0.038$ (17). All atoms were located with the exception of the methyl group hydrogens. Refinement in $P2_1$ appears unjustified since the atoms have acceptable thermal parameters with the exception of the more labile methyl group carbon atoms. Nonhydrogen atoms were refined with anisotropic thermal parameters and after location hydrogens were either located from difference Fourier maps or placed in geometrically idealized positions d(C–H) = 0.96 Å. Hydrogen atoms were refined with riding constraints and common isotropic thermal parameters were refined. Other details of the structure are given in Tables 2–5 and a listing of structure factor amplitudes was submitted as supplementary material.

TABLE 1
Structure Determination Summary for $3[NH_3CH_2CH_3][Al_3P_4O_{16}]$

Crystal data	
Empirical formula	$C_6H_{24}Al_3N_3O_{16}P_4$
Color; habit	Colorless bar
Crystal size (mm)	$0.1 \times 0.05 \times 0.05$
Crystal system	Monoclinic
Space group	$P2_1/m$ (No. 11)
Unit cell dimensions	$a = 8.920(2)$ Å
	$b = 14.896(2)$ Å
	$c = 9.363(2)$ Å
	$\beta = 106.07(2)°$
Volume	1191.6(4) $Å^3$
Z	2
Formula weight	599.1
Density (calc.)	1.66 Mg/m^3
Absorption coefficient	0.50 mm^{-1}
F (0 0 0)	616
Data collection	
Diffractometer used	Siemens P4-RA
Radiation	Mo$K\alpha$ ($\lambda = 0.71073$Å)
Temperature (K)	295
2θ range	3.0 to 47.0°
Scan type/speed	2θ–θ; 0.50 to 60.00°/min. in ω
Scan range (ω)	0.70° plus $K\alpha$ separation
Index ranges	$-9 \le H \le 9$, $-16 \le K \le 16$, $-10 \le L \le 1$
Reflections collected	3293
Independent reflections	1784 ($R_{int} = 2.23\%$)
Observation reflections	1384 ($F > 4.0\sigma(F)$)
Solution and refinement	
System used	Siemens SHELXTL IRIS
Solution	Direct Methods
Weighting scheme	$w^{-1} = \sigma^2(F) + 0.0002F^2$
Number of parameters refined	164
Final R indices (obs. data)	$R = 3.62\%$, $wR = 3.79\%$
R indices (all data)	$R = 5.61\%$, $wR = 4.36\%$
Goodness-of-fit	1.42
Largest and mean Δ/σ	0.001, 0.000
Data-to-parameter ratio	8.2:1
Largest difference peak/hole	0.45/−0.37 $eÅ^{-3}$

$R = \sum ||F_o| - |F_c|| / \sum |F_o|$
$wR = [\sum w(|F_o| - |F_c|)^2 / \sum |F_o|^2]^{1/2}$

TABLE 2
Atomic Coordinates and Equivalent Isotropic Displacement Coefficients ($Å^2$) for $3[NH_3CH_2CH_3][Al_3P_4O_{16}]$

	x	y	z	U_{eq}
$P(1)$	0.5134(2)	0.2500	0.7528(2)	0.017(1)
P!(2)	0.8586(2)	0.2500	0.4739(2)	0.017(1)
P(3)	0.3355(1)	0.0902(1)	0.3260(1)	0.017(1)
Al(1)	0.2107(2)	0.2500	0.4759(2)	0.015(1)
Al(2)	0.6561(1)	0.1100(1)	0.5837(1)	0.017(1)
O(1)	0.5077(5)	0.2500	0.9106(4)	0.031(2)
O(2)	0.7918(5)	0.2500	0.3089(5)	0.035(2)
O(3)	0.3325(3)	0.1015(2)	0.1670(3)	0.034(1)
O(4)	0.3503(5)	0.2500	0.6459(5)	0.034(2)
O(5)	1.0363(4)	0.2500	0.5210(5)	0.028(2)
O(6)	0.5993(3)	0.1668(2)	0.7223(3)	0.032(1)
O(7)	0.8090(3)	0.1667(2)	0.5454(3)	0.029(1)
O(8)	0.5015(3)	0.1044(2)	0.4244(3)	0.033(1)
O(9)	0.2270(3)	0.1557(2)	0.3726(3)	0.031(1)
O(10)	0.2809(3)	−0.0041(2)	0.3545(3)	0.031(1)
N(1)	0.2275(6)	0.2500	−0.0041(6)	0.032(2)
C(10)	0.0614(9)	0.2500	−0.0922(9)	0.057(3)
C(11)	−0.0405(11)	0.2500	0.0094(13)	0.135(7)
N(2)	0.6371(5)	0.1152(3)	0.1291(4)	0.040(1)
C(20)	0.7278(9)	0.0347(6)	0.1277(10)	0.108(4)
C(21)	0.7943(20)	−0.0070(7)	0.2490(14)	0.236(10)

Note. Equivalent isotropic U defined as one third of the trace of the orthogonalized U_{ij} tensor.

TABLE 3
Bond Lengths (Å) for $3[NH_3CH_2CH_3][Al_3P_4O_{16}]$

P(1)–O(1)	1.492(5)	P(1)–O(4)	1.521(4)
P(1)–O(6)	1.525(3)	P(1)–O(6′)	1.525(3)
P(2)–O(2)	1.494(4)	P(2)–O(5)	1.523(4)
P(2)–O(7)	1.533(3)	P(2)–O(7′)	1.533(3)
P(3)–O(3)	1.492(3)	P(3)–O(8)	1.527(3)
P(3)–O(9)	1.521(3)	P(3)–O(10)	1.534(3)
Al(1)–O(4)	1.728(4)	Al(1)–O(9)	1.734(3)
Al(1)–O(5) b	1.721(5)	Al(1)–O(9)′	1.734(3)
Al(2)–O(6)	1.738(3)	Al(2)–O(7)	1.724(3)
Al(2)–O(8)	1.730(3)	Al(2)–O(10) c	1.720(3)
N(1)–C(10)	1.482(8)	C(10)–C(11)	1.486(16)
N(2)–C(20)	1.449(9)	C(20)–C(21)	1.286(14)

Note. Equivalent isotropic U defined as one third of the trace of the orthogonalized U_{ij} tensor.

RESULTS AND DISCUSSION

Characterization of APO-TE

APO-TE exhibits an X-ray powder diffraction pattern that does not correspond to any known compound. A powder pattern generated from the single crystal analysis by the SHELXTL program XPOWD shows a close correspondence to that determined experimentally (18), indicating the individual crystal specimen chosen is representative of the whole sample. The crystals (Fig. 1) appear as rectangular bars with dimensions of ca. (40–60) × (45–75) × (80–120) μm.

TABLE 4
Bond Angles (°) for $3[NH_3CH_2CH_3][Al_3P_4O_{16}]$

O(1)–P(1)–O(4)	111.3(3)	O(1)–P(1)–O(6)	110.0(1)
O(4)–P(1)–O(6)	108.4(1)	O(1)–P(1)–O(6)′	110.0(1)
O(4)–P(1)–O(6)′	108.4(1)	O(6)–P(1)–O(6)	108.7(3)
O(2)–P(2)–O(5)	112.6(3)	O(2)–P(2)–O(7)	111.8(1)
O(5)–P(2)–O(7)	106.1(1)	O(2)–P(2)–O(7)′	111.8(1)
O(5)–P(2)–O(7)′	106.1(1)	O(7)–P(2)–O(7)′	108.2(3)
O(3)–P(3)–O(8)	109.5(2)	O(3)–P(3)–O(9)	112.1(2)
O(8)–P(3)–O(9)	109.0(2)	O(3)–P(3)–O(10)	111.0(2)
O(8)–P(3)–O(10)	108.9(2)	O(9)–P(3)–O(10)	106.3(2)
O(4)–Al(1)–O(9)	111.3(1)	O(4)–Al(1)–O(5) b	104.1(2)
O(9)–Al(1)–O(5) b	111.0(1)	O(4)–Al(1)–O(9)′	111.3(1)
O(9)–Al(1)–O(9)′	108.1(2)	O(5A)–Al(1)–O(9)′	111.0(1)
O(6)–Al(2)–O(7)	109.1(1)	O(6)–Al(2)–O(8)	109.9(2)
O(7)–Al(2)–O(8)	109.4(2)	O(6)–Al(2)–O(10) c	109.3(2)
O(7)–Al(2)–O(10) c	108.4(1)	O(8)–Al(2)–O(10) c	110.7(1)
P(1)–O(4)–Al(1)	156.9(3)	P(2)–O(5)–Al(1) d	150.2(3)
P(1)–O(6)–Al(2)	143.2(2)	P(2)–O(7)–Al(2)	145.9(2)
P(3)–O(8)–Al(2)	159.2(2)	P(3)–O(9)–Al(1)	146.9(2)
P(3)–O(10)–Al(2) c	143.9(2)	N(1)–C(10)–C(11)	109.7(7)
N(2)–C(20)–C(21)	120.9(10)		

Note. Equivalent isotropic U defined as one third of the trace of the orthogonalized U_{ij} tensor.

TABLE 5
Hydrogen Bond Contracts (Å)

N(1)----O(2)	2.827	N(1)----O(4)	2.740
N(2)----O(2)	2.871	N(2)----O(3)	2.736
N(2)----O(4)	2.843		

Note. Atoms generated by the following symmetry elements:
1. ′: x, $0.5 - y$, z
2. a: x, y, $z - 1$
3. b: $x - 1$, y, z
4. c: $1 - x$, $-y$, $1 - z$
5. d: $1 + x$, y, z

The IR spectrum of the compound exhibits three strong bands at 1082, 794–617, and 569–484 cm^{-1}, which are characteristic of aluminophosphates containing four- and six-membered rings (19, 20). The following vibrational assignments are also the suggested asymmetric stretching vibrations of the P–O–Al units at 1082 cm^{-1} and the symmetric stretching vibrations of the P–O–Al units at 794, 709, 646, and 618 cm^{-1}. Bands at 569, 520, and 484 cm^{-1} are also believed to rise from the bending vibrations of P–O units. Bands from the template cation $[CH_3CH_2NH_3]^+$ are also seen (21) at 1659 and 1560 cm^{-1} due to δ_{N-H} (in-plane) of $-NH_3^+$, at 1398 cm^{-1} assigned to the symmetric stretching vibration of $-CH_3$, and at 738 cm^{-1} for δ_{C-H} of $-CH_2-$. TGA–DTA curves show that the ethylammonium ions of APO-TE are lost during an endothermic change at ca. 270°C, consistent with the strong hydrogen bonding found in the structure. XRD shows that the compound has transformed into amorphous when the temperature is over 300°C, corresponding to the result of TGA–DTA. TGA shows a weight loss of 21.0% (weight) in agreement with the formula $[Al_3P_4O_{16}]^{3-} \cdot 3[CH_3CH_2NH_3]^+$ (23.0% (weight)) determined by single-crystal analysis. The P/Al obtained from ICP analysis is 1.34 and that from EDAX is 1.3 which are both close to the 1.33 value expected based on the P/Al integer ratio 4:3. Elemental analysis indicates that the C, N, and H contents are 12.15, 7.21, and 4.03% (weight), respectively, corresponding to a molar ratio C:H:N = 1.00:3.98:0.51. The analysis results are also in accordance with the formula of $[Al_3P_4O_{16}]^{3-} \cdot 3[CH_3CH_2NH_3]^+$.

Description of the Structure

The atomic coordinates and equivalent isotropic thermal parameters, interatomic distances, and angles are listed in Tables 2, 3, and 4, respectively. APO-TE consists of macroanionic sheets of the empirical formula $[Al_3P_4O_{16}]^{3-}$ separated by $[CH_3CH_2NH_3]^+$ cations. The sheets lie in the crystallographic *ab* plane (Fig. 2) are built up from vertices sharing AlO_4 and PO_4 tetrahedral units. Whereas all the AlO_4 vertices are shared by adjacent PO_4 units, leading to

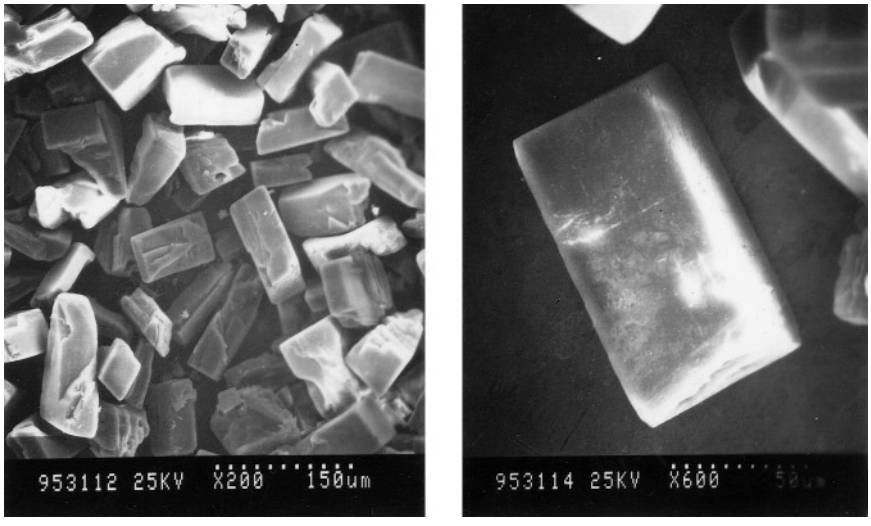

FIG. 1. Scanning electron micrograph of APO-TE crystals.

a P/Al ratio of 4/3, only three of the PO_4 vertices are linked to adjacent AlO_4 units, with those remaining corresponding to the P=O groups. The latter point above and below the mean plane of the sheet (Fig. 3). The AlO_4 and PO_4 tetrahedra are alternatively connected, giving puckered strands of Al_2P_2 four-membered rings, which are cross linked every third unit by the additional $P(2)O_4$ to form capped chair style six-membered rings and elliptic eight-membered rings which have pore size of ca. 3.8×6.0 Å. This sheet is similar to that previously described in the compound $[Al_3P_4O_{16}]^{3-} \cdot 1.5[NH_3CH_2CH_2NH_3]^{2+}$ (7).

The fundamental building block of the sheet is thus an Al_3P_4 unit consisting of a six-member Al_3P_3 ring capped by the additional phosphate group $P(1)O_4$. A similar building block is found in $[Al_3P_4O_{16}]^{3-} \cdot 3[NH_3(CH_2)_3CH_3]^{+}$ and $[Al_3P_4O_{16}]^{3-} \cdot 1.5[NH_3(CH_2)_4NH_3]^{2+}$, but these are connected in a different manner to form a sheet with 4, 6, and 12 membered rings (8, 9).

The asymmetric unit of the structure is shown in Fig. 4 with an atomic labeling scheme and contains the formula unit $1.5[NH_3CH_2CH_3][Al_{1.5}P_2O_8]$. There are three crystallographically independent P atoms, two Al positions, and 10 oxygen positions, however of these, two P, one Al, and four oxygens lie on the crystallographic mirror plane at $y = 0.2500$ and thus contribute just for 1/2 atom to the asymmetric unit. The environments of the two Al sites are topologically different but chemically similar, each being tetrahedrally coordinated by four O atoms, with Al–O

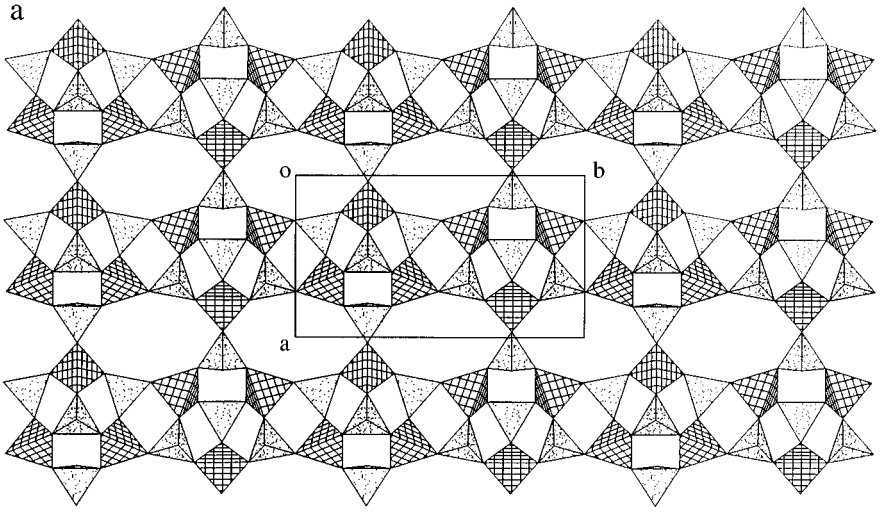

FIG. 2. View normal to the plane of the layer (a) and view along the layer plane for the compound (b) and (c).

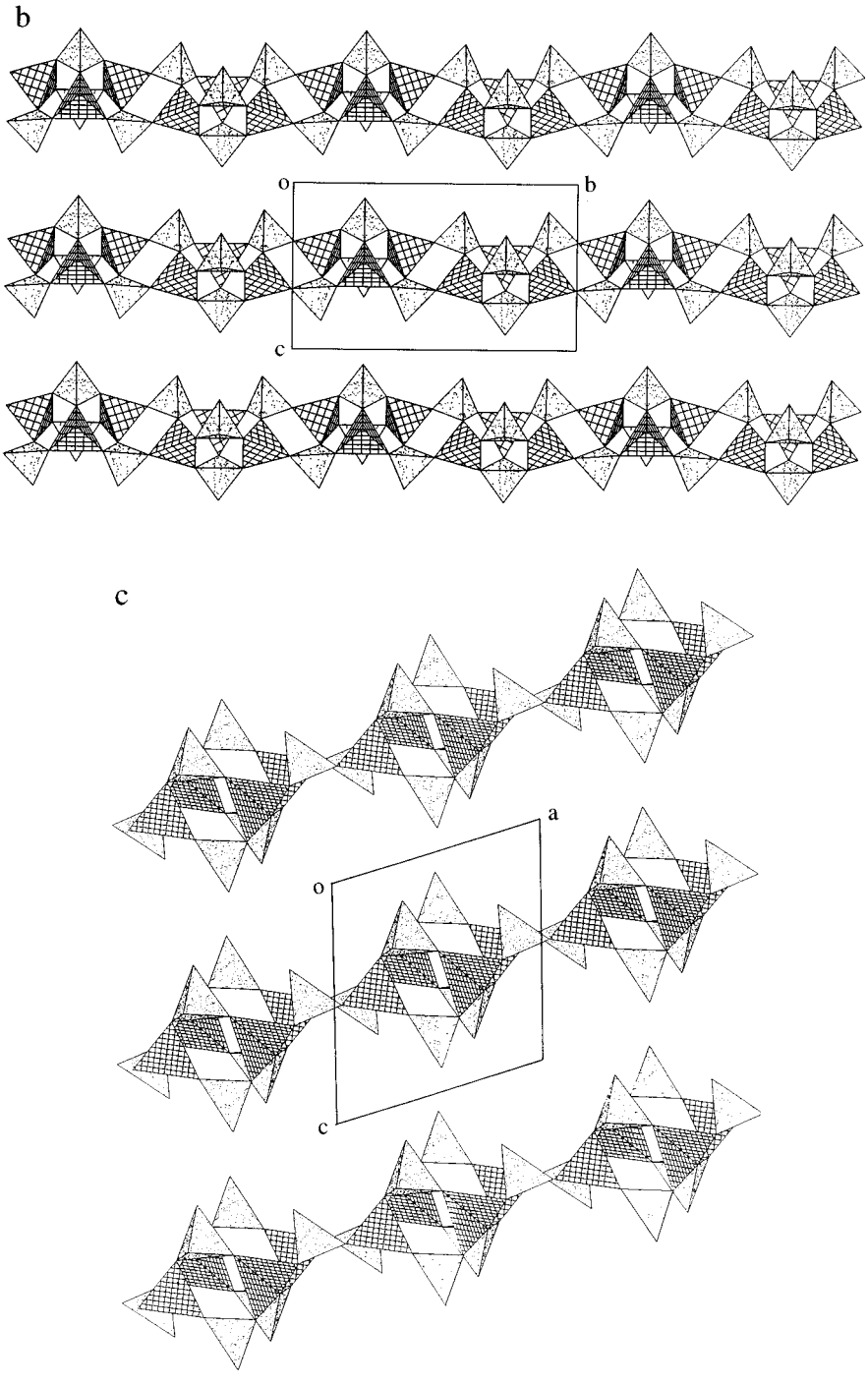

FIG. 2—*Continued*

contacts of 1.720–1.731 Å and O–Al–O angles between 104.1 and 111.3°. These values are in good agreement with those found in the mineral Berlinite (22). For each of the three PO_4 tetrahedra three of their coordinating oxygens bridge to Al atoms and have P–O bond lengths in the range 1.520–1.534 Å. The remaining P–O linkages, namely P(1)–O(1), P(2)–O(2), and P(3)–O(3) have lengths of 1.492–1.494 Å and may be considered formally as P=O double bonds. These distances are consistent with those of the terminal P=O groups in $H_3PO_4 \cdot 0.5H_2O$ of 1.485 and 1.495 Å (23). The multiple nature of the P=O bonds also influences the bond angles about phosphorous; all the

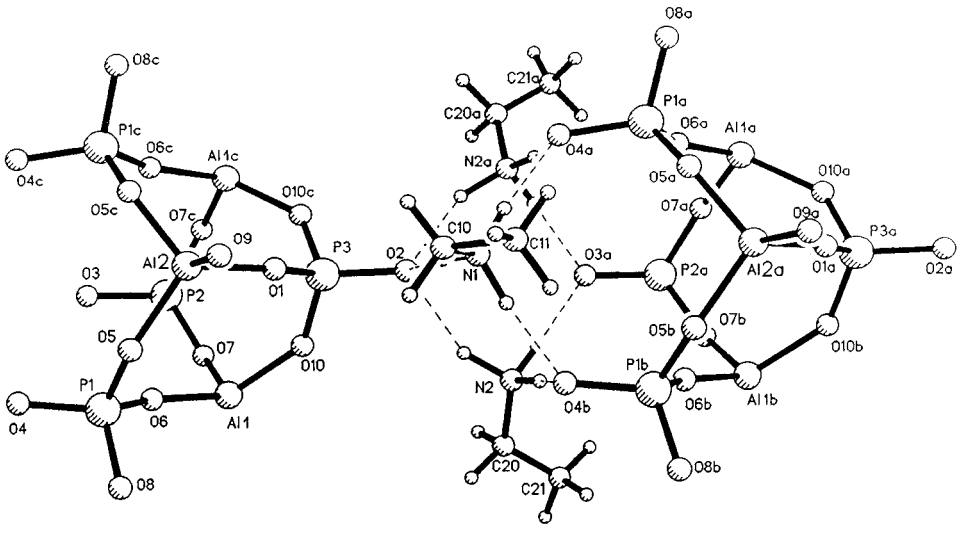

FIG. 3. View of the six-membered ring showing the symmetric character of P and Al atoms; view of the template between the two (top and bottom) six-membered rings showing the hydrogen bonds of the template ions and terminal P=O groups.

O–P–O angles (106.3–109.0°) are less than the O–P=O angles (109.5–112.6°) as expected from elementary VSEPR theory.

Figure 4 shows in plane view, the network of hydrogen bonds from each Al_3P_4 unit (Table 5) to the associated three ethylammonium cations. Each P=O group serves as multiple hydrogen bond acceptors. The $[NH_3CH_2CH_3]^+$ ions possibly help to promote the formation of the Al_3P_3 six-membered ring through the formation of six H-bonds

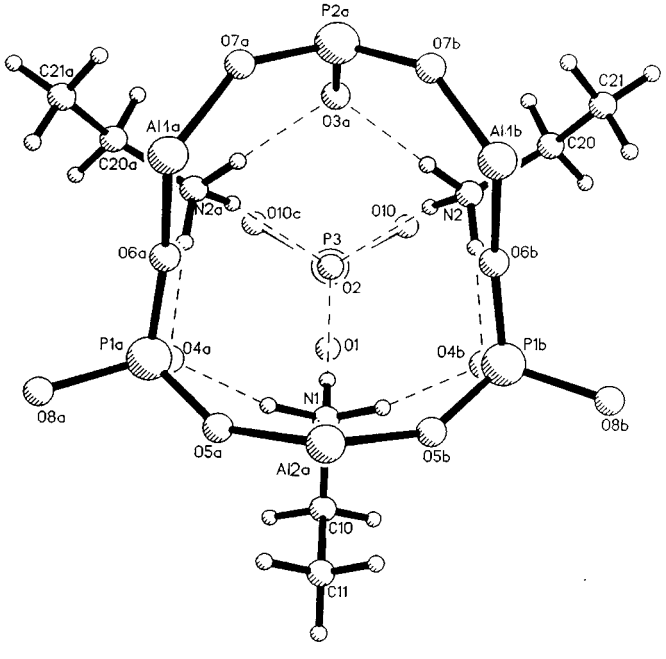

FIG. 4. View the template linked with the layers showing the layers are linked by hydrogen bonds of the template ions and the terminal P=O groups.

(N(1)–H--O(3), N(2)–H--O(2), and N(2)–H--O(3) and their mirror related counterparts). All three ethylammonium ions are also hydrogen bonded to P(1)=O(1) of the next sheet translated along the *z* axis, which serves to center this group in the middle of the Al_3P_3 ring and place it in perfect registry with the capping P(1)–O(1) of the adjacent sheet. Thus a stacking sequence of *AAAA* is set up by the H-bond network. This is in contrast to the *ABAB* sequence set by the difunctional $[NH_3CH_2CH_2NH_3]^{2+}$ (7). The compound possesses eight-membered ring channels along the *a* axis owing to the ethylammonium cations being about right under the bottom of the six-membered rings and the layers stacking in an *AAAA* sequence. This means that this unusual material has the character of 2-D aluminophosphate layers and 3-D aluminophosphate molecular sieves.

Relation among the Templates, the Structure of the Layers, and, the Sequences of the Stacking

To date, the major 2-D macroanion $[Al_3P_4O_{16}]^{3-}$ has been found to form two types of layers. Each possesses $[Al_3P_4]$ units of capped six-membered rings, however these can be functionally connected in different ways to yield $4 \times 6 \times 8$ nets (as for APO-TE) or $4 \times 6 \times 12$ nets. In addition the sequence of stacking between adjacent layers can either be of *AAAA* or *ABAB* type. We have found all four combinations of network and stacking sequence in the closely related family of organoammonium and diammonium salts $[NH_3R]$ and $[NH_3RNH_3]$ ($R = C_2$–C_4 alkyl). Interestingly the type of network appears to be influenced by the chain length of the cation and the stacking sequence by the mono- or bifunctionality of the cations (Fig. 5). The reasons for this stem from the subtleties of the hydrogen bond networks

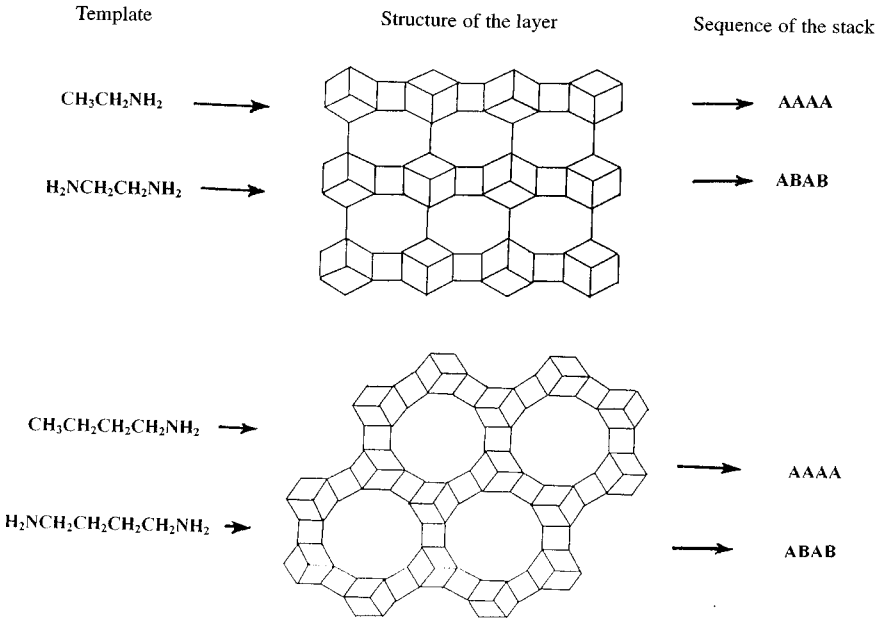

FIG. 5. The relation between the template and the structure of the layer and the relation between the template and the sequence of the stack for the layers.

which can be assumed to be thermodynamically slightly preferred compared to the more open $4 \times 6 \times 12$ which has large pore size. A $4 \times 6 \times 8$ network is formed using ethylammonium as template whereas the use of butylammonium leads to a structure $4 \times 6 \times 12$ of the macroanionic sheet. This critical changeover is also seen in the diammonium family when $[NH_3CH_2CH_2NH_3]^{2+}$ is replaced by the longer chain $[NH_3(CH_2)_4NH_3]^{2+}$ dication. Although the same system of H-bonds can be formed with the six-membered rings and the P=O groups, in progressing to *n*-butyl groups, the value of the counterions has increased. This extra steric bulk could be taken up to some extent by slightly increasing the separation between adjacent sheets, however packing efficiency and hydrophobic interactions are optimized if the net is changed to $4 \times 6 \times 12$. In this case the butyl tails are extended toward the 12 membered ring. The change over to a difunctional cation means that the H-bond network is modified so that the capping P=O groups are no longer in registry but translationally staggered from one sheet to the next.

In all the compounds characterized, the H-bond network is centered on the six-membered ring with its set of three P=O hydrogen-bond acceptors of one sheet. It seems likely that these types of terminal ammonium ions thus can promote formation of this unit which is conveniently capped by an additional phosphate group to yield the key building block of the sheet.

Other macroanions such as $[Al_2P_3O_{12}]^{3-}$ can also form layered materials as reported in the literature (15). However the constrains of connectivity are likely to limit the number of stoichiometries which can be found in the family of anionic aluminophosphates.

APPENDIX

TABLE 6
Anisotropic Displacement Coefficients (Å$\times 10^3$) for $3[NH_3CH_2CH_3][Al_3P_4O_{16}]$

	U_{11}	U_{22}	U_{33}	U_{12}	U_{13}	U_{23}
P(1)	14(1)	20(1)	16(1)	0	5(1)	0
P(2)	12(1)	17(1)	23(1)	0	7(1)	0
P(3)	19(1)	11(1)	20(1)	2(1)	4(1)	0(1)
Al(1)	11(1)	13(1)	21(1)	0	6(1)	0
Al(2)	15(1)	12(1)	24(1)	0(1)	5(1)	1(1)
O(1)	35(3)	44(3)	19(2)	0	13(2)	0
O(2)	39(3)	39(3)	22(3)	0	2(2)	0
O(3)	40(2)	39(2)	25(2)	−1(1)	11(2)	−1(1)
O(4)	19(2)	52(3)	27(3)	0	0(2)	0
O(5)	15(2)	33(2)	39(3)	0	12(2)	0
O(6)	38(2)	26(2)	35(2)	10(1)	16(2)	0(1)
O(7)	18(2)	29(2)	43(2)	−3(1)	12(2)	9(1)
O(8)	22(2)	39(2)	34(2)	−3(1)	2(1)	2(1)
O(9)	32(2)	21(2)	43(2)	6(1)	14(2)	−7(1)
O(10)	26(2)	15(1)	52(2)	2(1)	10(2)	7(1)
N(1)	28(3)	40(3)	29(3)	0	11(3)	0
C(10)	49(5)	69(6)	45(5)	0	1(4)	0
C(11)	37(6)	280(18)	90(9)	0	20(6)	0
N(2)	41(2)	47(2)	31(2)	−5(2)	11(2)	−8(2)
C(20)	95(6)	88(6)	120(8)	31(5)	−7(6)	−65(5)
C(21)	418(24)	95(8)	154(11)	149(12)	12(14)	2(8)

Note. The anisotropic displacement factor exponent takes the form $-2\pi^2(h^2a^{*2}U_{11} + \cdots + 2hka^*b^*U_{12})$.

TABLE 7
H-Atom Coordinates and Isotropic Displacement Coefficients ($Å^2$) for $3[NH_3CH_2CH_3][Al_3P_4O_{16}]$

	x	*y*	*z*	*U*
H(1A)	0.2958	0.2500	− 0.0566	0.063(8)
H(1B)	0.2514	0.1942	0.0488	0.063(8)
H(10A)	0.0386	0.1972	− 0.1547	0.136(19)
H(11A)	− 0.1503	0.2500	− 0.0432	0.372(46)
H(11B)	− 0.0159	0.1970	0.0711	0.372(46)
H(2A)	0.6186	0.1505	0.0355	0.063(8)
H(2B)	0.6841	0.1584	0.1881	0.063(8)
H(2C)	0.5379	0.1102	0.1624	0.063(8)
H(20A)	0.8148	0.0546	0.0943	0.136(19)
H(20B)	0.6674	− 0.0053	0.0533	0.136(19)
H(21A)	0.8555	− 0.0564	0.2307	0.372(46)
H(21B)	0.8583	0.0313	0.3239	0.372(46)
H(21C)	0.7089	− 0.0294	0.2824	0.372(46)

ACKNOWLEDGMENTS

The authors thank the National Natural Science Foundation of China for financial support.

REFERENCES

1. D. M. Bibby and M. P. Dale, *Nature* **317,** 157 (1985).
2. Q. Huo and R. Xu, *J. Chem. Soc., Chem. Commun.* 783 (1990).
3. Q. Gao, S. Li, and R. Xu, *J. Chem. Soc., Chem. Commun.* 1465 (1994).
4. A. M. Chippindale, A. V. Powell, R. H. Jones, J. M. Thomas, A. K. Cheetham, Q. Huo, and R. Xu, *Acta Crystallogr. C* **50,** 1537 (1994).
5. M. Light, M. B. Hursthouse, J. Yu, J. Chen, and R. Xu, submitted for publication.
6. A. M. Chippindale, A. V. Powell, L. M. Bull, R. H. Jones, A. K. Cheetham, J. M. Thomas, and R. Xu, *J. Solid State Chem.* **96,** 199 (1992).
7. R. H. Jones, J. M. Thomas, R. Xu, Q. Huo, A. K. Cheetham, and A. V. Powell, *J. Chem. Soc., Chem. Commun.* 1266 (1991).
8. A. M. Chippindale, Q. Huo, R. H. Jones, J. M. Thomas, R. Walton, and R. Xu, *J. Solid State Chem.* in press.
9. J. M. Thomas, R. H. Jones, R. Xu, J. Chen, A. M. Chippindale, S. Natarajan, and A. K. Cheetham, *J. Chem. Soc., Chem. Commun.* 929 (1992).
10. A. M. Chippindale, S. Natarajan, J. M. Thomas, and R. H. Jones, *J. Solid State Chem.* **111,** 18 (1994).
11. I. D. Williams, Q. Gao, J. Chen, L. Ngai, Z. Lin, and R. Xu, *J. Chem. Soc., Chem. Commun.* 1781 (1996).
12. R. H. Jones, J. M. Thomas, J. Chen, R. Xu, Q. Huo, S. Li, and Z. Ma, *J. Solid State Chem.* **102,** 204 (1993).
13. Q. Huo and R. Xu, *J. Chem. Soc., Chem. Commun.* 1391 (1992).
14. A. Kuperman, S. Nadimi, S. Oliver, G. A. Ozin, J. M. Garces, and M. M. Olken, *Nature* **365,** 239 (1993).
15. Q. Gao, J. Chen, S. Li, R. Xu, J. M. Thomas, M. Light, and M. B. Hurthouse, *J. Solid State Chem.* in press.
16. R. H. Jones, J. M. Thomas, R. Xu, Q. Huo, Y. Xu, A. K. Cheetham, and D. Bieber, *J. Chem. Soc., Chem. Commun.* 1170 (1990).
17. G. M. Shelddrick, *Acta Crystallogr. A* **46,** 467 (1990).
18. N. P. C. Walker and D. Stuart, *Acta Crystollogr. A* **39,** 158 (1983).
19. R. A. van Nordstrand, D. S. Santilli, and S. I. Zones, *ACS Symp. Ser.* **368,** 236 (1988).
20. M. E. Davis, C. Montes, P. E. Hathaway, J. P. Arhancet, D. L. Hasha, and J. M. Garces, *J. Am. Chem. Soc.* **111,** 3919 (1989).
21. Q. Jin, *Instrument Analysis*, Chap. II. *Jilin University*, 1990.
22. D. Schwarzenbach, *Z. Kristallogr.* **123,** 161 (1966).
23. B. Dickens, E. Prince, L. W. Schroeder, and T. H. Jordan, *Acta. Crystallogr. Struct. Crystallogr. Chem.* **1330,** 1470 (1974).